British Journal of Pharmacology

British Journal of Pharmacology (2016) **173** 2506–2520 2506

RESEARCH PAPER

The α7 nicotinic receptor dual allosteric agonist and positive allosteric modulator GAT107 reverses nociception in mouse models of inflammatory and neuropathic pain

Correspondence Dr Deniz Bagdas, Department of Pharmacology and Toxicology, Medical College of Virginia Campus, Virginia Commonwealth University, Richmond, VA 23298-0613, USA; and Dr Ganesh A. Thakur, Department of Pharmaceutical Sciences, Northeastern University, Boston, MA 02115, USA. E-mail: deniz.bagdas@vcuhealth.org; dbagdas@uludag.edu.tr; g.thakur@neu.edu

Received 20 October 2015; **Revised** 5 May 2016; **Accepted** 17 May 2016

Deniz Bagdas[1,2,*], Jenny L Wilkerson[1,*], Abhijit Kulkarni[3], Wisam Toma[1], Shakir AlSharari[1,4], Zulfiye Gul[5], Aron H Lichtman[1], Roger L Papke[6], Ganesh A Thakur[3] and M Imad Damaj[1]

[1]Department of Pharmacology and Toxicology, Medical College of Virginia Campus, Virginia Commonwealth University, Richmond, VA, USA, [2]Experimental Animals Breeding and Research Center, Faculty of Medicine, Uludag University, Bursa, Turkey, [3]Department of Pharmaceutical Sciences, Northeastern University, Boston, MA, USA, [4]Department of Pharmacology and Toxicology, King Saud University, Riyadh, Saudi Arabia, [5]Department of Pharmacology, Faculty of Medicine, Uludag University, Bursa, Turkey, and [6]Department of Pharmacology and Therapeutics, University of Florida, Gainesville, FL, USA

*Authors contributed equally to the paper.

BACKGROUND AND PURPOSE

Orthosteric agonists and positive allosteric modulators (PAMs) of the α7 nicotinic ACh receptor (nAChR) represent novel therapeutic approaches for pain modulation. Moreover, compounds with dual function as allosteric agonists and PAMs, known as ago-PAMs, add further regulation of receptor function.

EXPERIMENTAL APPROACH

Initial studies examined the α7 ago-PAM, GAT107, in the formalin, complete Freund's adjuvant (CFA), LPS inflammatory pain models, the chronic constriction injury neuropathic pain model and the tail flick and hot plate acute thermal nociceptive assays. Additional studies examined the locus of action of GAT107 and immunohistochemical markers in the dorsal horn of the spinal cord in the CFA model.

KEY RESULTS

Complementary pharmacological and genetic approaches confirmed that the dose-dependent antinociceptive effects of GAT107 were mediated through α7 nAChR. However, GAT107 was inactive in the tail flick and hot plate assays. In addition, GAT107 blocked conditioned place aversion elicited by acetic acid injection. Furthermore, intrathecal, but not intraplantar, injections of GAT107 reversed nociception in the CFA model, suggesting a spinal component of action. Immunohistochemical evaluation revealed an increase in the expression of astrocyte-specific glial fibrillary acidic protein and phosphorylated p38MAPK within the spinal cords of mice treated with CFA, which was attenuated by intrathecal GAT107 treatment. Importantly, GAT107 did not elicit motor impairment and continued to produce antinociceptive effects after subchronic administration in both phases of the formalin test.

CONCLUSIONS AND IMPLICATIONS

Collectively, these results provide the first proof of principle that α7 ago-PAMs represent an effective pharmacological strategy for treating inflammatory and neuropathic pain.

Abbreviations

CCI, chronic constriction nerve injury; CFA, complete Freund's adjuvant; GFAP, astrocyte-specific glial fibrillary acidic protein; i.pl., intraplantarly; KO, knockout; MLA, methyllycaconitine; nAChRs, nicotinic ACh receptors; PAM, positive allosteric modulator; p-p38MAPK, phosphorylated p38MAPK; WT, wild-type

DOI:10.1111/bph.13528

Tables of Links

TARGETS	
Ligand-gated ion channels[a]	**Enzymes**[b]
nAChRs	p38MAPK
α7 nAChR	

LIGANDS		
Acetic acid	IL-1β	Methyllycaconitine
ACh	Formalin	Naloxone
Choline	LPS	

These Tables list key protein targets and ligands in this article which are hyperlinked to corresponding entries in http://www.guidetopharmacology.org, the common portal for data from the IUPHAR/BPS Guide to PHARMACOLOGY (Southan *et al.*, 2016) and are permanently archived in the Concise Guide to PHARMACOLOGY 2015/16 ([a,b]Alexander *et al.*, 2015a,b).

Introduction

Neuronal nicotinic ACh receptors (nAChR) are recognized targets for drug development in several preclinical models of cognitive and neuro-degenerative disorders (Dziewczapolski *et al.*, 2009; Thomsen *et al.*, 2010). Along with their well-documented roles in cognition, nAChR activation produces analgesic effects in laboratory animal and human studies (Umana *et al.*, 2013). The homomeric α7 nAChR subtype is abundantly expressed in the CNS and periphery (Girod *et al.*, 1999). While activation of α7 nAChRs by orthosteric agonists induces antinociceptive effects in several experimental models of pain (Damaj *et al.*, 2000; Wang *et al.*, 2005; Feuerbach *et al.*, 2009; Bagdas *et al.*, 2011), these approaches may bring forward limitations, such as low probability of channel opening and rapid desensitization (Feuerbach *et al.*, 2009; Williams *et al.*, 2011). New approaches for the activation of α7 nAChRs have led to the identification of α7-selective positive allosteric modulators (PAMs) that circumvent the limitations of ligands that directly activate α7 nAChRs (Williams *et al.*, 2011) as well as a new class of agents identified as α7 'silent agonists' (Papke *et al.*, 2014a, 2015).

Recently, several structurally distinct and selective α7 nAChR PAMs were developed (Hurst *et al.*, 2005; Timmermann *et al.*, 2007). These PAMs were shown to increase the potency and/or maximal efficacy of endogenous (ACh and choline) or exogenous agonists for the α7 nAChRs. These α7 PAMs were active in mouse and rat models of chronic and inflammatory pain (Munro *et al.*, 2012; Freitas *et al.*, 2013a,b,c; Bagdas *et al.*, 2015b). In addition, α7 drugs for chronic pain and inflammation indications may not be ion channel activators but rather 'silent agonists', which bind to the receptor but preferentially induce non-conducting states that modulate signal transduction (Papke *et al.*, 2015).

While PAMs are thought to bind to a distinct binding site from the orthosteric site and lack intrinsic agonist activation, recent studies have reported that some molecules show dual activity, namely, allosteric modulators and allosteric agonists (Gill *et al.*, 2012; Thakur *et al.*, 2013). These molecules are described as ago-allosteric ligands or ago-PAMs. Accordingly, the present study investigated the antinociceptive properties of the recently reported ago-PAM compound, GAT107 (Thakur *et al.*, 2013; Papke *et al.*, 2014b). GAT107 is a potent α7 nAChR type II PAM with intrinsic allosteric agonist activities (Thakur *et al.*, 2013). We therefore tested and characterized GAT107 in mouse models of acute and chronic pain that mimic different pain modalities in humans. Its analgesic-like properties in acute (thermal spinal and supraspinal), tonic (formalin) inflammatory (both chemical and bacterial) and neuropathic pain [chronic constriction nerve injury (CCI)] models were determined.

Previous studies report that the α7 nAChR is found within the CNS on astrocytes (Shen and Yakel, 2012), and modulation of astrocytic α7 nAChR leads to anti-inflammatory signalling cascades, as well as decreases in astrocyte activation shown by the astrocyte-specific glial fibrillary acidic protein (GFAP) (Liu *et al.*, 2012; Niranjan *et al.*, 2012; Di Cesare Mannelli *et al.*, 2015). It is now supported that glial activation, including astrocyte activation, within the dorsal horn of the spinal cord may also play a critical role in mediating pathological pain (Kim *et al.*, 2009; Wilkerson *et al.*, 2012a, b). Indeed, increased GFAP expression has been widely used as a cellular marker coincident with pathological pain (Schreiber *et al.*, 2008; Gao and Ji, 2010; Wilkerson *et al.*, 2012a,b). One major upstream signalling cascade that leads to the production and release of pro-inflammatory cytokines is the phosphorylation of p38MAPK. This phosphorylated p38MAPK (p-p38MAPK) plays a critical role in mechanical allodynia that involves the action of pro-inflammatory cytokines, including IL-1β (Ji and Suter, 2007; Ji *et al.*, 2009), and astrocyte-specific p-p38MAPK is sufficient to produce pathological pain states (Moon *et al.*, 2014). Thus, here, we determined if GAT107 would reverse alterations in immunoreactivity of GFAP and p-p38MAPK and within the dorsal horn of the spinal cord in mice treated with complete Freund's adjuvant (CFA).

Methods

Animals

Male adult (8–10 weeks of age) ICR mice obtained from Harlan Laboratories (Indianapolis, IN, USA) and male adult C57BL6/J mice from The Jackson Laboratory (Bar Harbor, ME, USA) were used throughout the study. Mice null for the α7 subunits (The Jackson Laboratory) and their wild-type (WT) littermates were bred in an animal care facility at Virginia Commonwealth University. For all experiments, mice were backcrossed for ≥8–10 generations. Mutant and WT mice were obtained by crossing heterozygote mice. This breeding scheme controlled for any irregularities that might occur with crossing solely mutant animals. Mice were housed in a 21°C humidity-controlled Association for Assessment

and Accreditation of Laboratory Animal Care-approved animal care facility. They were housed in groups of four and had free access to food and water. The rooms were on a 12 h light/dark cycle (lights on at 07:00 h). All experiments were performed during the light cycle (between 07:00 and 19:00 h), and the study was approved by the Institutional Animal Care and Use Committee of Virginia Commonwealth University. All studies were carried out in accordance with the National Institutes of Health's Guide for the Care and Use of Laboratory Animals. Animals were killed via CO_2 following by cervical dislocation after the experiments finished, unless noted otherwise. Any subjects that subsequently showed behavioural disturbances unrelated to the pain induction procedure were excluded from further behavioural testing. Animal studies are reported in compliance with the ARRIVE guidelines (Kilkenny *et al.*, 2010; McGrath and Lilley, 2015).

Behavioural assessments

Formalin test. The formalin test was carried out in an open Plexiglas cage (29 × 19 × 13 cm each). Mice were allowed to acclimatize for 15 min in the test cage prior to injection. Each animal was injected with 20 μL of (2.5%) formalin to the right hind paw i.pl. Mice were observed from 0 to 5 min (phase I) and 20 to 45 min (phase II) post-formalin injection. The amount of time spent licking the injected paw was recorded with a digital stopwatch. Paw diameter (see the Measurement of paw oedema section) was also measured before and 1 h after formalin injection.

GAT107 (0.1, 1, 3 and 10 mg·kg^{-1}) or vehicle was injected i.p. 15 min before formalin injection. For the antagonist studies, the α7 nicotinic antagonist MLA (10 mg·kg^{-1}), opiate antagonist naloxone (2 mg·kg^{-1}) or vehicle (saline) was injected s.c. 15 min before the GAT107 (10 mg·kg^{-1}, i.p.) or vehicle injection. In a separate group, GAT107 (10 mg·kg^{-1}, i.p.) effects in the formalin test were measured in α7 WT and knockout (KO) mice.

For the subchronic GAT107 administration study, mice were administered GAT107 (1 and 10 mg·kg^{-1}, i.p.) or vehicle for 6 days twice daily with 8 h apart and were challenged with GAT107 (1 or 10 mg·kg^{-1}, i.p.) on day 7 and tested in formalin test. A vehicle control group, in which mice were exposed to 7 days of vehicle, was also included.

CFA-induced inflammatory pain model. Mice were injected i.pl. with 20 μL of CFA (50%, diluted in mineral oil). Mechanical allodynia (see measurement of von Frey test) and thermal hyperalgesia (see Hargreaves test) were measured before and 3 days after CFA injection. GAT107 (1, 3 and 10 mg·kg^{-1}) or vehicle was injected i.p. on day 3 after CFA injection and tested for possible anti-allodynic and antihyperalgesic efficacy. Antagonist studies were performed as described above.

We also determined the contribution of spinal α7 nAChR mediation in the effects of GAT107 using i.t. injection of MLA in a separate cohort of mice. For this reason, we injected MLA (10 μg 5 μL^{-1} per mouse, i.t.) or its vehicle 15 min before GAT107 (10 mg·kg^{-1}, i.p.) or its vehicle. Mice were tested for allodynia 15 min after the last injection.

In order to test whether GAT107 produced its antinociceptive effects through a spinal or peripheral site of action, drugs were administered i.t. or i.pl. respectively. For spinal studies, GAT107 (0.3 and 3 μg 5 μL^{-1} per mouse) or vehicle (5% DMSO) were injected i.t. 3 days after the CFA injection. For peripheral studies, GAT107 (3 and 9 μg 20 μL^{-1} per mouse) or vehicle (1:1:18) was injected i.pl. Mechanical allodynia was then tested at different time points, and paw diameter was measured 1 h after GAT107 injection.

In a separate experiment, we performed immunohistochemistry of GFAP and p-p38MAPK staining in the dorsal horn of the spinal cord 3 days after the CFA or its vehicle injection. We examined whether i.t. GAT107 would reduce the increase oinGFAP and p-p38MAPK in the dorsal horn of the spinal cord. For this study, CFA or mineral oil (vehicle of CFA) was injected to the right hind paw. After 3 days, GAT107 (3 μg 5 μL^{-1} per mouse) or vehicle (5% DMSO) was injected i.t. to the CFA and mineral oil-treated mice. Mechanical thresholds were measured before CFA or its vehicle, on the test day (3 days after) and after 2 h from GAT107 or its vehicle i.t. injection. Following determination of the last mechanical threshold, mice were immediately overdosed with vaporized isoflurane, perfused, and tissues harvested for immunohistochemical procedures.

LPS-induced inflammatory pain model. Inflammatory pain was induced by injecting 2.5 μg LPS from *Escherichia coli* 026:B6 (Sigma) in 20 μL of physiological saline into the plantar surface of the right hind paw of each mouse. The LPS dose used in this study does not produce oedema (Booker *et al.*, 2012). Mice were returned to their home cages after LPS injection for a 22 h period before commencing all experiments. On the test day, GAT107 (1, 3 and 10 mg·kg^{-1}) or vehicle was injected i.p., and the animals were tested for mechanical allodynia.

CCI-induced neuropathic pain model. Mice were anaesthetized with pentobarbital (45 mg·kg^{-1}, i.p.). An incision was made just below the hip bone, parallel to the sciatic nerve. The left common sciatic nerve was exposed at the level proximal to the sciatic trifurcation, and a nerve segment 3–5 mm long was separated from the surrounding connective tissue. Two loose ligatures with 5–0 silk suture were made around the nerve with a 1.0–1.5 mm interval between each of them. Muscles were closed with suture thread and the wound with wound clips. This procedure resulted in CCI of the ligated nerve. GAT107 (1, 3 and 10 mg·kg^{-1}) or vehicle was injected i.p. 2 weeks after CCI surgery, and the animals were tested for changes in thermal hyperalgesia and mechanical allodynia.

Evaluation of thermal hyperalgesia and mechanical allodynia. Thermal hyperalgesia was measured via the Hargreaves test as described before (Bagdas *et al.*, 2015a). Three measures of paw withdrawal latency were taken and averaged for each hind paw using the Hargreaves test. Results are expressed either as withdrawal latency for each paw or as ΔPWL (in s) = contralateral latency − ipsilateral latency.

Mechanical allodynia thresholds were determined according to the method of Chaplan *et al.* (1994 and as adapted in Bagdas *et al.* (2015a. A series of calibrated von Frey filaments (Stoelting, Wood Dale, IL, USA) with logarithmically incremental stiffness ranging from 2.83 to 5.07 expressed as

dsLog10 of (10 lb force in mg) were applied to the paw with a modified up-down method (Dixon, 1965). The mechanical threshold was expressed as Log10 of (10 lb force in mg), indicating the force of the von Frey hair to which the animal reacted (paw withdrawn, licking or shaking). All behavioural testing on animals was performed in a blinded manner.

Measurement of paw oedema. The thickness of the formalin- or CFA-treated paws was measured both before and after injections at the time points indicated above, using a digital calliper (Traceable Callipers, Friendswood, TX, USA). Data were recorded to the nearest ±0.01 mm and expressed as change in paw thickness (ΔPD = difference in the ipsilateral paw diameter before and after injection paw thickness).

Acetic acid-induced writhing test. For the measurement of acetic acid-induced nociceptive behaviour, each mouse was placed in a Plexiglas box and allowed to acclimatize for 20 min. Then the mouse was given an i.p. injection of acetic acid (1%) or saline at a total volume of 1 mL 100 g^{-1} body weight and then returned to the box. Counting the number of typical writhing behaviours started immediately after acetic acid administration, and the number of stretches (a stretch was operationally defined as a contraction of the abdomen followed by an extension of the hind limbs) was recorded in 10 min bins for a total of 60 min. Experiments were carried out by injecting the mice with either vehicle or GAT107 (1, 3 and 10 mg·kg^{-1}, i.p.), and 15 min later, they received acetic acid (1%) and were tested as described above.

Acetic acid-induced CPA. To evaluate the negative affective component of pain, the conditioned place aversion (CPA) test was performed as previously described (Papke *et al.*, 2015). In brief, separate groups of mice were handled for 3 days prior to initiation of CPA testing. On day 1, mice were placed in the grey centre compartment for a 5 min habituation period, followed by a 15 min test period of freely exploring all compartments to determine baseline responses. A baseline score was recorded and used to randomly pair each mouse with either the black or white compartment. Drug-paired sides were randomized so that an even number of mice received drug on the black and white side. On day 2 (conditioning session), conditioning was performed as follows: the mice were given an i.p. injection of saline as a control non-noxious stimulus or 1% acetic acid as a noxious stimulus at a total volume of 1 mL 100 g^{-1} body weight (for both saline and acetic acid) and then immediately confined in the drug-paired compartment for 40 min. In addition, mice were pretreated with vehicle (i.p.) or GAT107 (1, 3 and 10 mg·kg^{-1}, i.p.) 15 min prior to acetic acid or saline injection. On the test day (day 3), mice were allowed to freely explore all compartments, and the day 1 procedure was repeated. Data are expressed as time spent on the drug-paired side post-conditioning minus the time spent on the drug-paired side preconditioning. A positive number indicates preference for the drug-paired side, whereas a negative number indicates aversion to the drug-paired side. A number at or near zero indicates no preference for either side.

Acute thermal pain tests. The antinociceptive effect of GAT107 was assessed by the tail flick method of D'Amour and Smith (1941 as modified by Dewey *et al.* (1970. Antinociceptive response was calculated as the percentage maximum possible effect (%MPE), where %MPE = {[(test value − control value)/(cut-off (10 s) − control value)] * 100}. The antinociceptive effect of GAT107 was also assessed in the hot plate test (Thermojust Apparatus, Columbus, OH, USA) maintained at 55°C. Antinociceptive response was calculated as %MPE, where %MPE = {[test value − control]/[cut-off time (40 s) − control] * 100}. The reaction time was recorded when the animal jumped or licked its paws. Experiments were carried out by injecting the mice with either vehicle or GAT107 (10 mg·kg^{-1}, i.p.), and animals were tested 15, 30, 45 and 60 min after injection.

Locomotor activity test. Mice were placed into individual Omnitech photocell activity cages (28 × 16.5 cm) (Columbus, OH, USA). Interruptions of the photocell beams (two banks of eight cells each) were recorded for the next 30 min. Data are expressed as the number of photocell interruptions.

Motor coordination. The effects of drugs on motor coordination were measured using the rotarod test (IITC Inc., Life Science, Woodland Hills, CA, USA) as previously described (Freitas *et al.*, 2013a). The impairment was calculated as follows: % impairment = (180 − test time)/(180 * 100). Mice were pretreated with either i.p. vehicle or GAT107 (10 mg·kg^{-1}, i.p.) 15 min before the test.

Intrathecal (i.t.) injections

Injections were performed free hand between the fifth and sixth lumbar vertebra in unanaesthetized mice according to the method of Hylden and Wilcox (1980).

Immunohistochemical procedures from CPA-treated mice

Mice were overdosed with vaporized isoflurane and then perfused transcardially with saline followed by 4% paraformaldehyde. Whole vertebral columns with intact spinal cords (cervical 2 through sacral 1 spinal column segments) were removed and underwent overnight fixation in 4% paraformaldehyde at 4°C. All specimens underwent EDTA (Sigma Aldrich) decalcification for 20 days, and spinal column sections were subsequently treated with paraffin, embedded, sliced and mounted on slides, as previously described (Wilkerson *et al.*, 2012a,b).

Slides were treated for immunohistochemistry for the detection of GFAP and p-p38MAPK, as previously described (Wilkerson *et al.*, 2012a,b). Briefly, slides were incubated with primary antibody overnight at 4°C, in a humidity chamber, and incubated with a fluorophore-conjugated secondary antibody for 2 h the following day. For the detection of p-p38MAPK, slides were incubated with biotinylated secondary antibody for 1 h and then treated with Vectastain ABC Elite kit (Vector Labs, Burlingame, CA, USA) and stained using TSA Plus Fluorescein System (PerkinElmer Life Sciences, Waltham, MA, USA) to allow for signal amplification. Slides were cover slipped with Vectashield containing DAPI (Vector Labs).

Image J software analysis

Fluorescent images for standard fluorescence analysis were obtained in the same manner as detailed above and analysed as previously described (Wilkerson *et al.*, 2012b). Briefly, images were taken on a Zeiss AxioImager Z2 fluorescence microscope (Carl Zeiss, AG, Germany). Images were then converted to grey scale and analysed using Image J software available for free download at http://rsb.info.nih.gov/ij/. Briefly, a total of four tissue sections from a single animal were averaged to obtain an individual animal's overall fluorescent intensity, with four animals in each experimental treatment group, to generate an average for that experimental condition. Likewise, background values were generated from control tissues incubated with PBS and the given secondary antibody and averaged together. The average background was then subtracted from the above mentioned average of each experimental treatment group.

Statistical analysis

The data obtained were analysed using the GraphPad software, version 6.0 (GraphPad Software, Inc., La Jolla, CA, USA), and expressed as the mean ± SEM. Statistical analysis was done using the one-way or two-way ANOVA test, followed by the *post hoc* Tukey's test. Student's unpaired *t*-test was used for spontaneous activity and motor coordination. The P values <0.05 were considered significant. The data and statistical analysis comply with the recommendations on experimental design and analysis in pharmacology (Curtis *et al.*, 2015).

Drugs

Methyllycaconitine (MLA) citrate was purchased from RBI (Natick, MA, USA). Naloxone was obtained from the National Institute for Drug Abuse (Rockville, MD, USA). Acetic acid, carrageenan, CFA and DMSO were purchased from Sigma-Aldrich (St. Louis, MO, USA). GAT107 ((3aR,4S,9bS)-4-(4-bromophenyl)-3a,4,5,9b-tetrahydro-3*H*-cyclopenta[c] quinoline-8-sulfonamide) was synthesized as described previously (Kulkarni and Thakur, 2013; Thakur *et al.*, 2013). GAT107 was dissolved in a mixture of 1:1:18 [1 volume ethanol/1 volume Emulphor-620 (Rhone-Poulenc, Inc., Princeton, NJ, USA)/18 volumes distilled water] and administered i.p. for systemic injections and intraplantarly (i.pl.) for peripheral injections. GAT107 was dissolved in 5% DMSO for intrathecal (i.t.) injection experiments. Other drugs were dissolved in physiological saline (0.9% sodium chloride) and injected s.c. at a total volume of 1 mL 100 g^{-1} body weight, unless noted otherwise. All doses are expressed as the free base of the drug.

Results

Acute GAT107 dose-dependently attenuates phase II formalin-induced pain and oedema

As seen in Figure 1A, GAT107 did not significantly affect nociceptive behaviour during phase I [$F_{(4,25)}$ = 1.913, P = 0.90]. However, it dose-dependently attenuated nociceptive behaviour in phase II [$F_{(4,25)}$ = 8.231, $P < 0.001$]. In addition, GAT107 significantly reduced paw oedema [$F_{(3,23)}$ = 9.345, $P < 0.001$; Figure 1B], with mice treated with 3 and 10 mg·kg^{-1} doses differing from the vehicle group.

We next explored the possible role of α7 nAChRs and opioid receptors in the effect of GAT107 in phase II of the formalin test. As shown in Figure 1C, a significant effect of treatment was found [$F_{(5,30)}$ = 40.82, $P < 0.001$]. Neither antagonist given alone significantly affected nociceptive behaviour (P = 0.72). While s.c. naloxone (2 mg·kg^{-1}) failed to reverse the effect of GAT107 (10 mg·kg^{-1}, i.p.) ($P > 0.05$), MLA (10 mg·kg^{-1}, s.c.) blocked the antinociceptive effect of GAT107 ($P < 0.001$). Furthermore, while GAT107 reduced formalin-induced paw licking in WT mice, the effect vanished in α7 KO mice [$F_{(1,20)}$ = 20.38, $P < 0.001$; interaction between drug and genotype; Figure 1D].

Subchronic GAT107 attenuates phase I and phase II formalin pain, without producing tolerance

In the next experiment, we investigated whether the antinociceptive effects of GAT107 in the formalin test would undergo tolerance after subchronic administration. GAT107 produced significant effects in phase I [$F_{(4,25)}$ = 5.842, $P < 0.01$; Figure 2A] and phase 2 [$F_{(4,25)}$ = 12.66, $P < 0.001$; Figure 2B]. In phase I, GAT107 failed to reduce paw licking behaviour in subchronic vehicle-treated mice ($P > 0.05$). Surprisingly, it induced antinociceptive behaviour in subchronic GAT107-treated mice ($P < 0.001$; Figure 2A). Furthermore, tolerance did not develop after subchronic exposure to GAT107 during phase II of the formalin test ($P < 0.001$; Figure 2B).

GAT107 dose-dependently attenuates CFA-induced inflammatory pain in an α7 nAChR-dependent manner

GAT107 dose-dependently reduced CFA-induced allodynia [$F_{\text{dosextime}(21,147)}$ = 5.969, $P < 0.01$; Figure 3A] and hyperalgesia [$F_{\text{dosextime}(12,84)}$ = 9.585, $P < 0.001$; Figure 3B). *Post hoc* analysis revealed that 10 mg·kg^{-1} GAT107 yielded maximal reversal similar to pretreatment baseline values at 15 to 30 min after injection. The anti-allodynic effects of 10 mg·kg^{-1} GAT107 lasted for 2 h, while the antihyperalgesic effects lasted for 1 h.

We next evaluated the possible role and site of α7 nAChRs in the antinociceptive effects of GAT107 in the CFA model. Both systemic (10 mg·kg^{-1}) [$F_{(3,20)}$ = 26.21, $P < 0.001$; Figure 3C] and spinal (10 μg/5 μL) [$F_{(3,20)}$ = 24.77, $P < 0.001$; Figure 3D] administration of the α7 nAChR antagonist MLA totally reversed the anti-allodynic effects of GAT107 (10 mg·kg^{-1}, i.p.). Similarly, MLA (10 mg·kg^{-1}, s.c.) blocked the antihyperalgesic effect of 10 mg·kg^{-1} GAT107 [$F_{(3,20)}$ = 22.82, $P < 0.001$; Figure 3E].

GAT107 has a central site of action and not peripheral

Figure 4 shows a comparison of spinal and peripheral administration of GAT107 (0.3 and 3 μg, i.t.; 3 and 9 μg, i.pl.) in the CFA test. Spinal GAT107 induced anti-allodynic effects in a dose-related manner [$F_{\text{dosextime}(14,70)}$ = 3.58, $P < 0.001$; Figure 4A]. GAT107 also reducedthe CFA-induced paw oedema at both doses [$F_{(2,15)}$ = 5.124,$P < 0.05$; Figure 4 B]. In contrast, i.pl. administration of GAT107 failed to show any significant anti-allodynic [$F_{\text{dose}(2,10)}$ = 0.20, P = 0.82] or

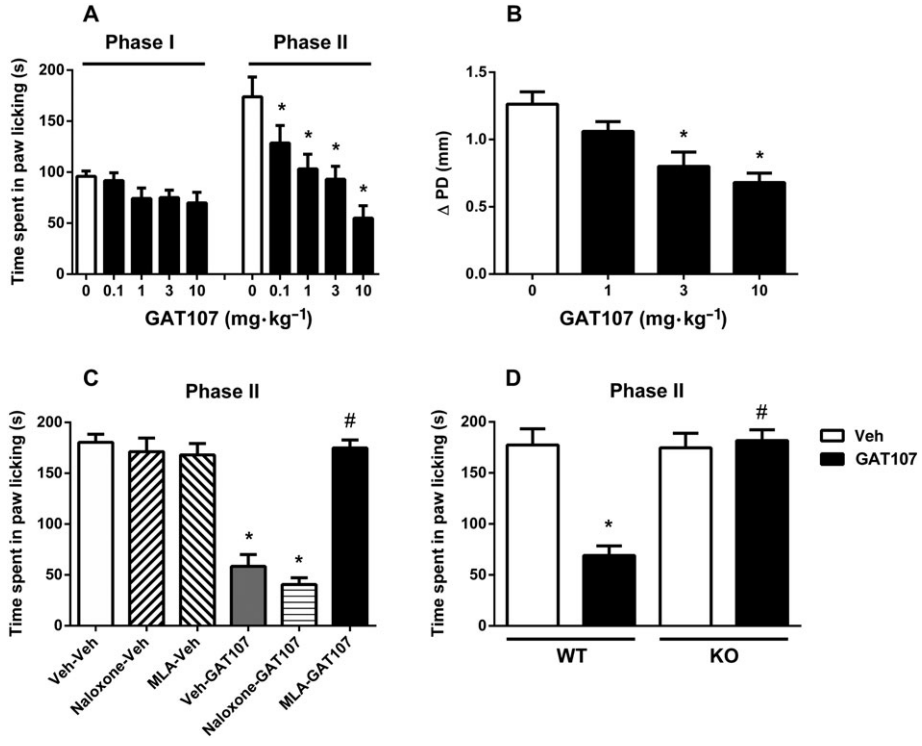

Figure 1

The antinociceptive and anti-oedema effects of GAT107 in the formalin test. (A) The effect after i.p. administration of GAT107 (0.1, 1, 3 and 10 mg·kg^{-1}) on formalin-induced pain behaviour in the mouse. Mice were treated with i.p. GAT107 15 min prior to formalin (2.5%, 20 μL) injection into the plantar region of the right hind paw. The cumulative pain response of time of licking was measured during the period of 0–5 (first phase) and 20–45 min (second phase). (B) Anti-oedema effect of GAT107 (1, 3 and 10 mg·kg^{-1}, i.p.) in the formalin test, as measured by the difference in the ipsilateral paw diameter before and after injection (ΔPD), 1 h after i.pl. injection of 2.5% formalin. (C) Blockade of the antinociceptive effect of GAT107 in the second phase of the formalin test by the α7 antagonist MLA citrate and opioid antagonist naloxone. MLA (10 mg·kg^{-1}, s.c.) and naloxone (2 mg·kg^{-1}, s.c.) were given 15 min before GAT107 (10 mg·kg^{-1}, i.p.) or vehicle (Veh). (D) Antinociceptive effects of GAT107 (10 mg·kg^{-1}, i.p.) in the second phase of the formalin test in the α7 WT and KO mice. Data are given as the mean ± SEM of six animals for each group in A, C and D. In (B) group sizes as follows: Veh ($n = 6$), GAT107 1 mg·kg^{-1} ($n = 7$), 3 mg·kg^{-1} ($n = 7$) and 10 mg·kg^{-1} ($n = 7$). The differences in experimental numbers within these studies reflect an odd number of animals evenly distributed in the experimental design. *$P < 0.05$, significantly different from its Veh group; #$P < 0.05$, significantly different from its corresponding control group (GAT107-treated group or WT group).

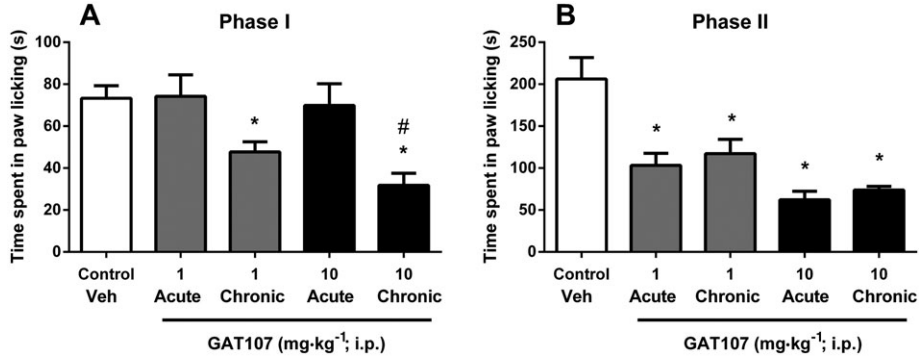

Figure 2

The antinociceptive effects of repeated administration GAT107 in the formalin test. The effect of GAT107 after subchronic i.p. administration of the drug on formalin-induced pain behaviour in the mouse. Mice were treated with GAT107 (1 and 10 mg·kg^{-1}, i.p.) or vehicle (Veh) for 6 days twice daily with 8 h apart and were challenged with GAT107 (1 and 10 mg·kg^{-1}, i.p.) on day 7 and effects evaluated in formalin (2.5%) test. A Veh control group, in which mice were exposed to 7 days of vehicle, was also included. The cumulative pain response of time of licking was measured during the period of 0–5 min first phase (A) and 20–40 min second phase (B). Data are given as the mean ± SEM of six animals for each group. *$P < 0.05$, significantly different from its Veh group. #$P < 0.05$, significantly different from acute group.

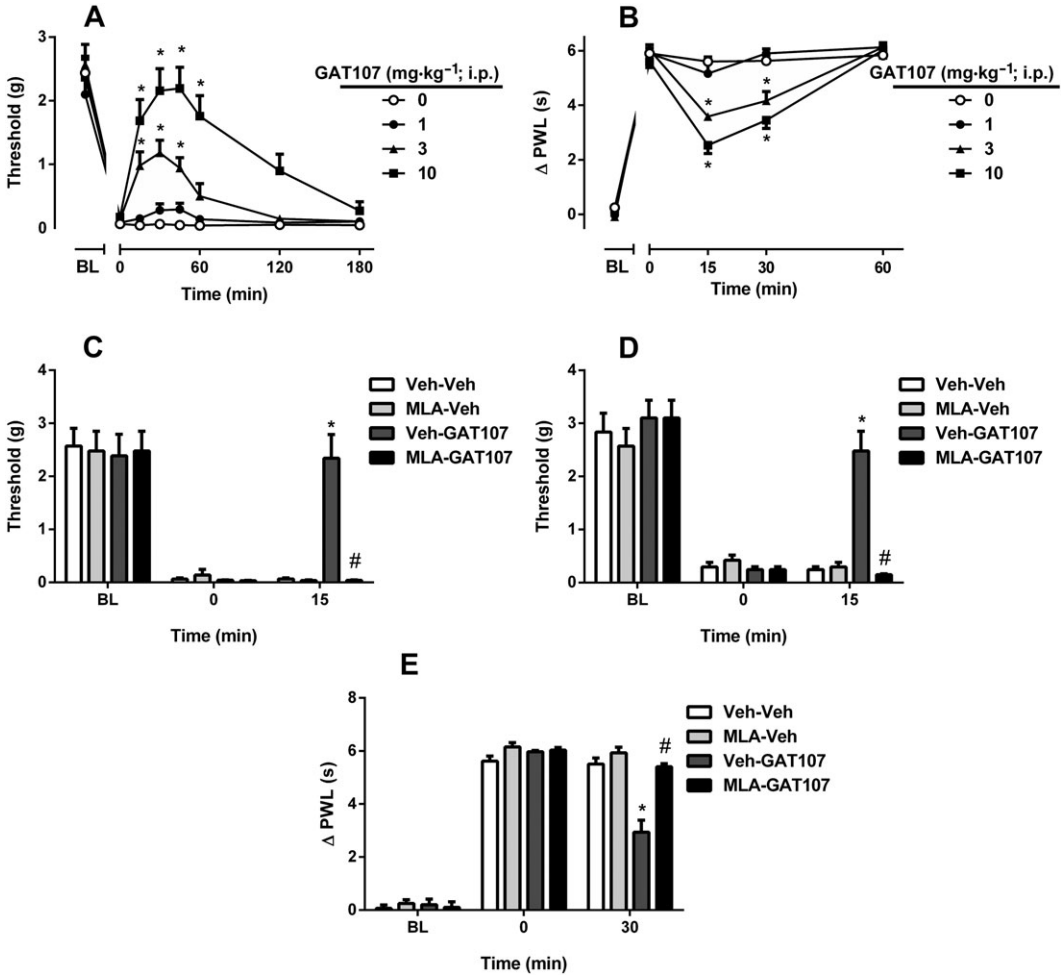

Figure 3

The anti-allodynic and antihyperalgesic effects of systemic GAT107 in the CFA-induced chronic inflammatory pain model. The (A) anti-allodynic and (B) antihyperalgesic effects of after i.p. administration of various doses of GAT107 (1, 3 and 10 mg·kg^{-1}). The mechanical paw withdrawal thresholds and differences in paw withdrawal latencies (ΔPWL = contralateral − ipsilateral hind paw latencies) were determined 3 days after i.pl. injection of CFA (50%). To determine the blockade of the anti-allodynic effect of GAT107 by the α7 antagonist MLA citrate, MLA was administered (C) systemically (10 mg·kg^{-1}, s.c.) and (D) spinal (10 μg in 5 μL, i.t.) 15 min before GAT107 (10 mg·kg^{-1}, i.p.) injection. (E) Blockade of the antihyperalgesic effects of GAT107 by MLA (10 mg·kg^{-1}, s.c.) in the Hargreaves test. Data are given as the mean ± SEM of eight animals for each group in A and B and six animals for each group in C, D and E. *$P < 0.05$, significantly different from its vehicle (Veh) group. #$P < 0.05$, significantly different from its corresponding control group (GAT107-treated group). BL, baseline.

anti-oedematous [$F_{(2,15)}$ = 2.2, P = 0.15] effects, even at the higher dose of 9 μg per mouse (Figure 4C and D).

GAT107 attenuates CFA-induced GFAP and p-p8MAPK activation in spinal cord dorsal horn

The above pharmacological studies identified the spinal cord as an important site for the effects of GAT107 in the CFA test. Accordingly, we next examined whether i.t. GAT107 would reduce CFA-induced phosphorylation of intracellular p38MAPK as well as the specific marker for astrocytic activation GFAP (Eng *et al.*, 2000) in the dorsal horn of the spinal cord. As shown in Figure 5A, while CFA reduced paw withdrawal thresholds, mineral oil (vehicle of CFA) did not alter mechanical thresholds 3 days following administration. GAT107 (3 μg per mouse, i.t.) attenuated CFA-induced reduction (Figure 5A). We did not perform the statistical analysis for the immunohistochemistry studies, because of the group size (n = 4 per group). Although statistical analysis was not conducted, there was a trend for GAT107 to reduce CFA-induced GFAP and p-p38MAPK immunoreactivity in the dorsal horn of the spinal cord.

Figure 5B shows that CFA-treated mice displayed a robust bilateral increase in dorsal horn GFAP immunoreactivity. i.t. administration of GAT107 attenuated CFA-induced astrocyte activation. GAT107 reduced the bilateral increases of GFAP immunoreactivity in dorsal horn (Figure 5B). Corresponding representative fluorescent images used for analysis are shown, vehicle (mineral oil)-injected mice treated with i.t. vehicle (5% DMSO) or CFA-treated mice injected with either i.t. GAT107 or equivolume vehicle (Figure 5B).

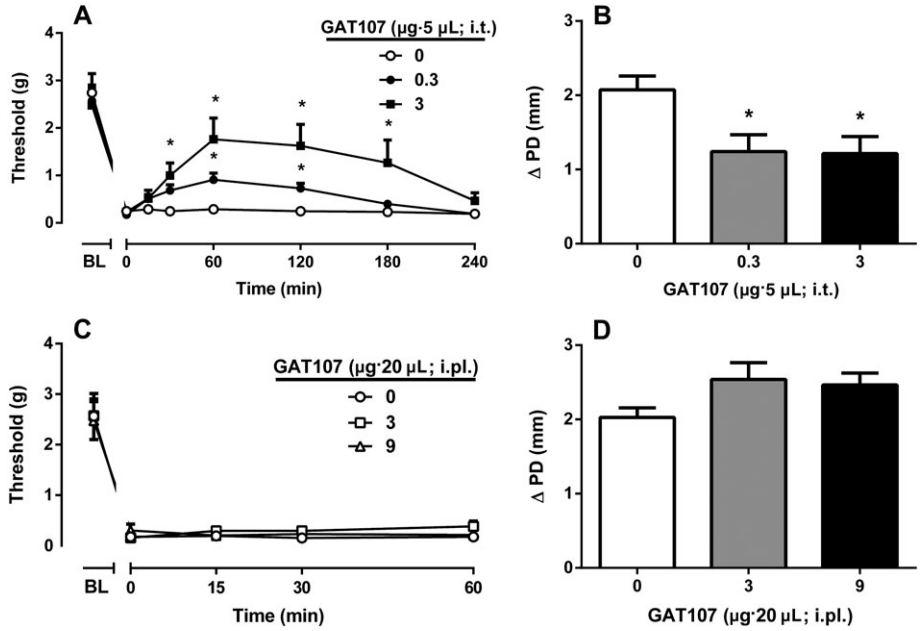

Figure 4

The anti-allodynic and anti-inflammatory effects of spinal and peripheral GAT107 in the CFA-induced chronic inflammatory pain model. A head-to-head comparison of anti-allodynic effects of (A) spinal (0.3 and 3 μg per mouse, i.t.) and (C) peripheral (3 and 9 μg per mouse, i.pl.) GAT107 in CFA-induced inflammatory pain. The anti-inflammatory effect of (B) spinal and (D) peripheral injection of GAT107, measured by the difference in the ipsilateral paw diameter before and after CFA injection (ΔPD), was assessed 1 h after GAT107 injection. Data are given as the mean ± SEM of six animals for each group in A and B. (C and D) Group sizes as follows: vehicle ($n = 5$), GAT107 3 μg ($n = 6$) and 9 μg ($n = 6$). The differences in experimental numbers within these studies reflect an odd number of animals evenly distributed in the experimental design. *$P < 0.05$, significantly different from its vehicle group. BL, baseline.

In addition, CFA produced a bilateral increase of p-p38MAPK immunoreactivity in dorsal horn. GAT107 (i.t.) reduced the bilateral increases of p-p38MAPK immunoreactivity in dorsal horn (Figure 5C). Again, representative fluorescent images are presented, which correspond to image analysis of vehicle-injected mice with i.t. vehicle, CFA-treated mice with i.t. vehicle or CFA-treated mice with GAT107 (Figure 5C). The figures are based on the studies referred in the Supporting Information.

GAT107 dose-dependently attenuates LPS-induced inflammatory pain

GAT107 dose-dependently reversed LPS-induced mechanical allodynia [$F_{dosextime(15,90)} = 3.762$, $P < 0.001$; Figure 6], with the dose of 10 mg·kg^{-1} producing complete blockade. *Post hoc* analysis revealed that the anti-allodynic effects of GAT107 were evident from 15 to 60 min after injection and returned to control by 120 min.

GAT107 dose-dependently attenuates CCI-induced neuropathic pain

The anti-allodynic and antihyperalgesic effects of GAT107 were explored in the CCI-induced neuropathic pain model. GAT107 dose-dependently and time-dependently reversed CCI-induced allodynia [$F_{dosextime(15,135)} = 9.29$, $P < 0.001$; Figure 7A]. However, GAT107 did not alter von Frey responses in sham-treated mice [$F_{dose(3,15)} = 0.28$, $P > 0.05$; Figure 7B].

Furthermore, GAT107 induced significant dose-related antihyperalgesic effects in CCI mice [$F_{dosextime(6,30)} = 6.622$, $P < 0.001$; Figure 7C] but not in the sham mice [$F_{dose(3,15)} = 0.40$, $P > 0.05$; Figure 7D].

GAT107 dose-dependently reduces acetic acid-induced writhings and CPA

GAT107 (3 or 10 mg·kg^{-1}) significantly reduced both acetic acid-induced nociceptive behaviours [$F_{(3,20)} = 16.25$, $P < 0.001$; Figure 8A]. Acetic acid (1%) induced CPA, which was prevented by pretreatment with GAT107 [$F_{(5,32)} = 2.649$, $P < 0.05$; Figure 8B]. *Post hoc* analysis revealed that 10 mg·kg^{-1} GAT107 blocked place aversion ($P < 0.001$).

GAT107 has no antinociceptive properties in acute thermal pain

In contrast to the other nociceptive assays, 10 mg·kg^{-1} GAT107 failed to show significant antinociceptive activity in the tail flick and hot plate tests [$F_{dose(1,10)} = 0.042$, $P > 0.05$, and $F_{dose(1,10)} = 2.232$, $P > 0.05$ respectively; Figure 9].

GAT107 does not alter motor activity and coordination

As seen in Table 1, mice treated with GAT107 (10 mg·kg^{-1}, i.p.) did not affect spontaneous activity or performance in the rotarod test ($t = 0.04698$, d.f. = 10, $P > 0.05$, and $t = 0.3359$, d.f. = 9, $P > 0.05$ respectively).

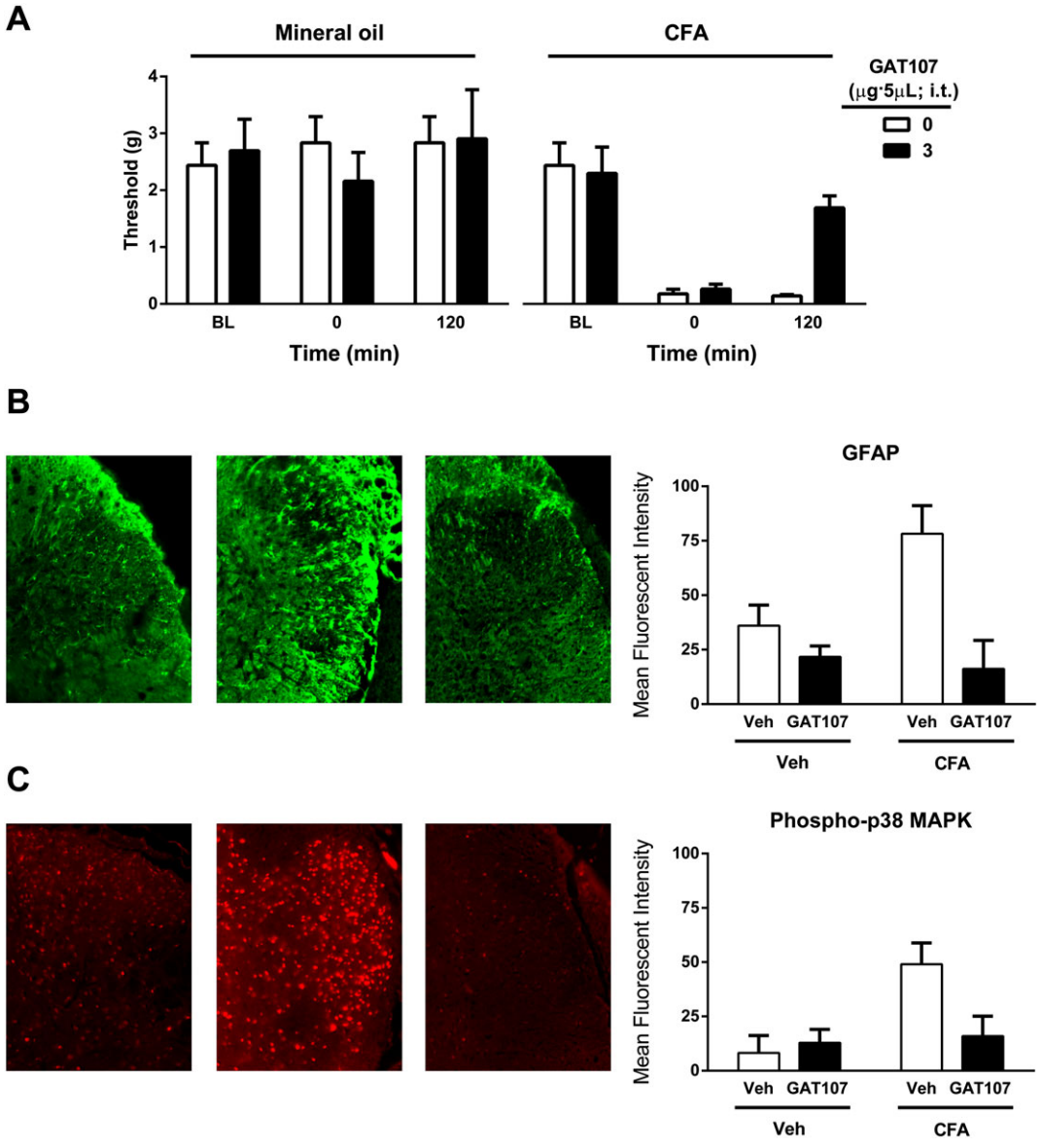

Figure 5

Immunoreactivity of GFAP and p-p38MAPK following GAT107-induced reversal of allodynia. (A) Prior to CFA injection, all groups exhibited similar baseline (BL) thresholds. CFA produced significant allodynia. Behavioural responses following i.t. GAT107 (3 μg) produced maximal reversal of allodynia. At peak reversal, animals were killed, and spinal tissue was collected. (B) Compared with vehicle (Veh)-injected mice given i.t. GAT107 or equivolume of Veh, CFA mice demonstrated a robust increase in dorsal horn GFAP immunoreactivity given i.t. Veh. Representative images at 20× magnification of GFAP fluorescent staining (green). (C) Compared with Veh-injected mice given i.t. GAT107 or equivolume Veh, CFA mice produced a robust p-p38MAPK increase in dorsal horn spinal cord tissues following i.t. Veh injection. GAT107 administered i.t. reversed CFA-induced increases in p-p38MAPK immunoreactivity. Representative images at 20× magnification of p-p38MAPK fluorescent staining (red). In all images, the scale bar is equal to 50 μm. Data are given as the mean ± SEM of four animals for each group.

Discussion

The recent discovery of compounds that can function as dual allosteric agonists and PAMs (ago-PAMs) add a new pharmacological approach for the regulation of α7 nAChR function (Gill *et al.*, 2011, 2012; Thakur *et al.*, 2013; Papke *et al.*, 2014b). In this concept, the identification of GAT107 (Thakur *et al.*, 2013) as an α7 ago-PAM provides a new approach for the treatment of chronic pain and inflammation. Our results establish the antinociceptive and anti-inflammatory efficacy of GAT107 in a battery of mouse models of pain. Similar to some α7 nAChR agonists (Gao *et al.*, 2010; Papke *et al.*, 2015) and PAMs (Freitas *et al.*, 2013a), GAT107 lacked activity in acute thermal pain tests (hot plate and tail flick). Importantly, no changes were seen in motor locomotion or coordination with antinociceptive doses of GAT107 in mice.

α7 nAChR-dependent antinociceptive activity results via interaction with the receptor by orthostatic agonists, PAMs or the more recently characterized dual ago-PAMs. Since

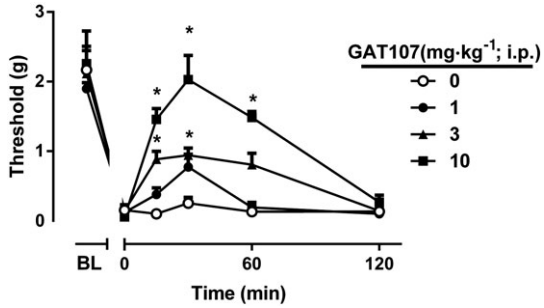

Figure 6

The anti-allodynic effects of GAT107 in LPS-induced inflammatory pain model. The anti-allodynic effects after i.p. administration of various doses of GAT107 (1, 3 and 10 mg·kg^{-1}). The mechanical paw withdrawal thresholds were determined 24 h after i.pl. injection of LPS (2.5 μg in 20 μL). Data are given as the mean ± SEM of seven animals for each group. *$P < 0.05$, significantly different from its vehicle group. BL, baseline.

there are limitations via direct agonist activation, such as low probability of channel opening and rapid desensitization (Williams *et al.*, 2011), PAMs provide antinociceptive action with less side effects. α7 nAChR PAMs have been classified as either type I, such as NS1738, or type II, such as PNU-120596, based on differences in their effect on desensitization (Bertrand and Gopalakrishnan, 2007; Timmermann *et al.*, 2007). Specifically, PAMs classified as type I predominantly affect the apparent peak current, with little effect on desensitization kinetics, whereas type II increase the apparent peak current and evoke a distinct weakly decaying current (Hurst *et al.*, 2005). Interestingly, while a type I PAM failed to produce an antinociceptive effect, a type II PAM induced long-lasting anti-allodynic effects (Freitas *et al.*, 2013b; Bagdas *et al.*, 2015b). While mainly PAMs have been described as allosteric modulators that lack direct agonist activity, ago-PAMs can produce both allosteric agonist activation and allosteric modulation of α7 nAChR function. Hence, the ago-PAMs of α7 nAChRs would be more efficacious in multiple and varied pain models. Indeed, the analgesic activity of GAT107 was assessed through various pain models including chemical, mechanical and thermal nociception assays, as well as chronic inflammatory and neuropathic pain models. Here, we show that GAT107 provides a wide spectrum of analgesic activity compared with other nicotinic ligands which show variations and limitations in their analgesic action (Gao *et al.*, 2010).

Our current results with GAT107 confirm previous studies and provide novel findings. To better evaluate the potential analgesic properties of GAT107, various mouse models of pain were chosen to mimic distinct clinical pain conditions and pathological etiologies. Here, we show that GAT107 is efficacious in chronic and inflammatory but not acute forms of pain. α7 nAChRs agonists show variable effects in acute pain assays where some of the ligands are active and others not (Hamurtekin and Gurun, 2006; Gao *et al.*, 2010; Freitas *et al.*, 2013a; Papke *et al.*, 2015). GAT107's activity on acute pain stimulus was consistent with our previous results with PAMs (Freitas *et al.*, 2013a; Bagdas *et al.*, 2015b).

GAT107 attenuated pain behaviour in the second phase of the formalin test, which is associated with the development of inflammation and spinal cord dorsal horn sensitization, but was ineffective in phase I (immediately after formalin injection), which is mediated by C-fibre activity (Abbott *et al.*, 1995; Davidson and Carlton, 1998). Moreover,

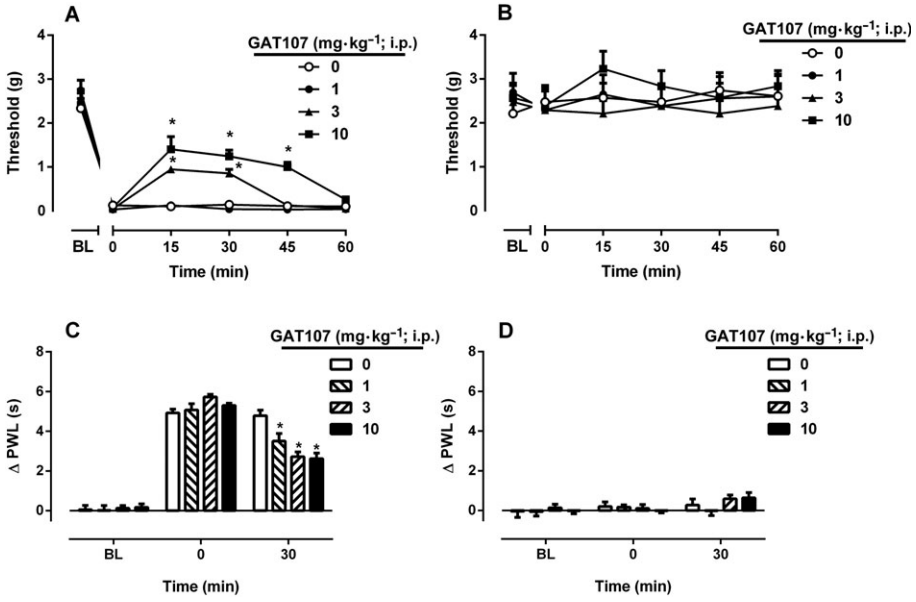

Figure 7

The anti-allodynic effects of GAT107 in CCI-induced neuropathic pain. The anti-allodynic effects after i.p. injection of GAT107 (1, 3 and 10 mg·kg^{-1}) in (A) CCI and (B) sham mice were determined using the von Frey test. The antihyperalgesic effects of GAT107 (1, 3 and 10 mg·kg^{-1}) were tested 30 min after its injection in (C) CCI and (D) sham mice using the Hargreaves test. Data are given as the mean ± SEM of 10 animals for each group in (A) and six animals for each group in (B, C and D). *$P < 0.05$, significantly different from its vehicle group. BL, baseline.

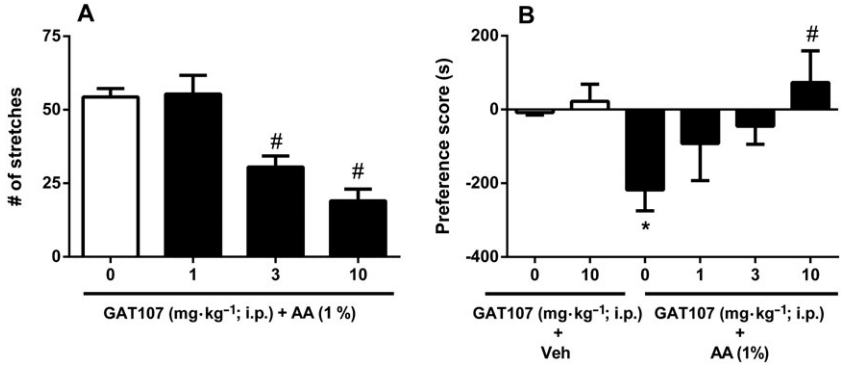

Figure 8

Effects of GAT107 on acetic acid (AA)-induced stretching and CPA. (A) i.p. injection of GAT107 (1, 3 and 10 mg·kg^{-1}) attenuated AA-induced writhing behaviour. (B) GAT107 (1, 3 and 10 mg·kg^{-1}, i.p.) attenuated AA-induced CPA. Data are given as the mean ± SEM of six animals for each group in (A). (B) Group sizes as follows: vehicle (Veh) and AA controls ($n = 7$) and others ($n = 6$). The differences in experimental numbers within these studies reflect an odd number of animals evenly distributed in the experimental design. *$P < 0.05$, compared with the Veh-injected mice; #$P < 0.05$, compared with the AA-injected mice.

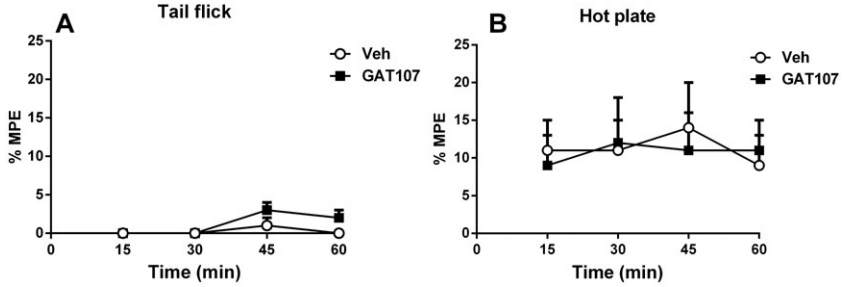

Figure 9

Effects of GAT107 in (A) the tail flick and (B) hot plate tests. The antinociceptive effects of GAT107 (10 mg·kg^{-1}, i.p.) were measured at multiple time points (in min) after injection. Data are presented as %MPE ± SEM of six animals for each group.

Table 1

Effects of GAT107 on motor activity and coordination of mice

Treatment	Spontaneous activity (# interrupts per 10 min)	Rotarod activity (% impairment)
Vehicle	743.8 ± 169.7	1.483 ± 0.8
GAT107	755.2 ± 171.4	1.120 ± 0.8

Mice were placed into photocell activity cages for 30 min or placed on the rotarod for 3 min after 15 min i.p. administration of GAT107. Data are presented as mean ± SEM as the number of photocell interruptions and time to fall in % impairment for each group respectively (5–6). The differences in experimental numbers within these studies reflect an odd number of animals evenly distributed in the experimental design.

GAT107 decreased formalin-induced paw oedema, consistent with the idea that it acts on the inflammatory phase of formalin test. In addition, repeated GAT107 administration not only maintained its antinociceptive effects during phase II of the formalin test but also significantly reduced nociceptive behaviours during phase I. The effectiveness of GAT107 exposure during phase I, therefore, may also be due to adaptive changes induced by repeated exposure to the drug or drug accumulation at the α7 nAChR. The results of the present study are consistent with our previous work showing that α7 nAChR PAMs produce antinociceptive effects in formalin test (Freitas *et al.*, 2013a,c).

To verify the selectivity of α7 nAChRs in GAT107's effects, we utilized complimentary genetic and pharmacological approaches, α7 KO mice and the α7-selective antagonist MLA. Using these approaches, we confirmed that the antinociceptive effects of GAT107 in the formalin test require α7 nAChRs. In order to minimize the number of animals

used, we tested the α7 antagonist MLA in only the formalin and CFA models and α7 KO mice in the formalin model. Additionally, the opioid receptor antagonist naloxone failed to reverse the antinociceptive effects of GAT107 in the formalin test, suggesting a lack of involvement of the opioid receptors.

To further address the selectivity of α7 nAChR activation by GAT107, we examined several anatomical sites where GAT107 may act to produce antinociceptive behavioural effects. GAT107 exhibited clear anti-allodynic and antihyperalgesic effects in the CFA model via spinal α7 nAChRs. Indeed, i.t. but not i.pl., GAT107 administration attenuated CFA-induced mechanical allodynia and paw oedema. These data suggest that GAT107 reverses mechanical allodynia through the central sites of action, namely, the spinal cord. Furthermore, the finding that MLA given i.t. completely blocked the anti-allodynic effects of systemically administered GAT107 suggests that spinal pain mechanisms may play an important role for the expression of the anti-allodynic effects of GAT107.

The spinal cord has previously been shown to be a key site where the molecular action of nAChRs produces analgesia. It has been reported that electrophysiological recordings from spinal cord slices show a strong nicotine-induced increase in inhibitory synaptic transmission, which was mediated partially by α4β2 and only minimally by α7 subtypes (Gao *et al.*, 2010). However, this previous report mainly focused on the actions of neuronal α7 nAChR and not glial α7 nAChR within the dorsal horn of the spinal cord. Other studies demonstrate that α7 nAChR activation produces neuroprotective effects (Shytle *et al.*, 2004; de Simone *et al.*, 2005; Nizri *et al.*, 2009; Liu *et al.*, 2012; Egea *et al.*, 2015). Here, we report that bilateral increases in both GFAP and p-p38MAPK immunoreactivity were observed in the dorsal horn of the spinal cord following injection of CFA. Spinal administration of GAT107 reversed CFA-induced allodynia and blocked the activation of both GFAP and p-p38MAPK in the spinal cord. One possible explanation of our findings is that spinal α7 nAChR activation leads to either direct or indirect decreases in astrocyte activation, leading to reductions in p-p38MAPK, ERK1/2 and downstream proinflammatory signalling molecules such as TNF-α (Moon *et al.*, 2014). This is supported by previous studies showing that PNU-120596 produces anti-inflammatory effects in rats via a decrease in TNF-α and IL-6 levels (Munro *et al.*, 2012) and GAT107 includes type II PAM properties. It is also possible that an α7-dependent regulation of cholinergic anti-inflammatory pathway (e.g. TNF-α through an NF-κB pathway) may mediate the antinociceptive effects of GAT107 (Bernik *et al.*, 2002). Although not examined here, it is important to note that α7 nAChR is expressed on microglia and macrophage (de Simone *et al.*, 2005; Su *et al.*, 2007; Takeda *et al.*, 2007) and microglial α7 nAChR is a key element in promoting neuroprotection (Shytle *et al.*, 2004; Parada *et al.*, 2013; Egea *et al.*, 2015; Yang *et al.*, 2015) and may contribute to the effects observed. More studies, outside the scope of this body of work, are needed to elucidate the full cellular mechanisms and contributions underlying the effects shown here. Taken together, these findings suggest that modulation of spinal cord glia, via α7 nAChRs, is sufficient to produce antinociceptive effects.

GAT107 dose-dependently inhibited acetic acid-induced CPA as well as acetic acid-induced abdominal stretching behaviour. GAT107 inhibition of CPA was not due to the rewarding properties of the drug since GAT107 alone did not induce a conditioned place preference. Our results are also consistent with α7 nAChR silent agonist NS6740 and α7 nAChR type II PAM 3-furan-2-yl-*N*-*p*-tolyl-acrylamide, which modulates the acetic acid-induced stretching behaviour and pain-related aversion (Papke *et al.*, 2015; Bagdas *et al.*, 2015b). These results suggest that α7 nAChR modulation may play an important role in dampening the aversive signs of pain.

GAT107 activity at α7 nAChRs has been shown to be regulated by aromatic amino acids that span the subunit interface (Papke *et al.*, 2014b). It has recently been reported that there are three distinct forms of GAT107 effects on the currents of *Xenopus* oocytes expressing human α7 nAChR: (1) direct activation, (2) direct potentiation obtained when GAT107 and ACh are together and (3) primed potentiation, which involves potentiation of agonist-evoked responses after GAT107 has been applied, with an intervening washout period prior to the agonist (e.g. ACh) application (Papke *et al.*, 2014b). Because α7 nAChR has an additional and potentially druggable site, molecules working at this direct allosteric activation site may allow fine-tuning over a broad range of pharmacological responses (Horenstein *et al.*, 2016). In this context, GAT107 may act more effectively than PAMs under appropriate conditions *in vivo*. While this may be due to GAT107's channel activating properties, it should also be noted that GAT107 has very prolonged effects on the conformational dynamics of the receptor, which are not manifested in its allosteric activation but rather in its ability to prime potentiation (Papke *et al.*, 2014b). When primed for potentiation, channels are closed, but receptors are in a unique conformation, which may impact the signal transduction through the protein's interactome (Paulo *et al.*, 2009), mediated by epitopes in the protein's poorly understood intracellular domain (Stokes *et al.*, 2015). The potential significance of stabilized non-conducting (desensitized) states for signal transduction is consistent with the effects of NS6740, a strongly desensitizing α7 silent agonist which has effects in these same pain models that are very similar to those of GAT107, in spite of the fact that it produces essentially no channel activation (Papke *et al.*, 2015). Since there are no published data with α7 nAChR ago-PAMs in pain, it is hard to separate the origin of the mechanisms in effects come from such agonist, PAM or both. On the other hand, we suggest that the GAT107 has a similar efficacy to an α7 nAChR mainly PAM in chronic pain (Munro *et al.*, 2012; Freitas *et al.*, 2013a; Freitas *et al.*, 2013b; Freitas *et al.*, 2013c; Bagdas *et al.*, 2015b) and it has lack of activity in acute thermal pain tests similar to some α7 nAChR agonists (Gao *et al.*, 2010; Papke *et al.*, 2015) and PAMs (Freitas *et al.*, 2013a). Therefore, further work is needed to dissect the *in vivo* impact of allosteric activation from allosteric modulation functions of ago-PAMs.

In conclusion, this study is the first to demonstrate the anti-inflammatory and antinociceptive actions of the α7 ago-PAM GAT107 in mouse models of chronic inflammatory and neuropathic pain. Furthermore, our current observations emphasize the important role of spinal α7 nAChRs as well as astrocytic mechanisms in the dorsal spinal horn in GAT107 effects. Overall, these results suggest that targeting α7 nAChRs with ago-PAMs represents a promising therapeutic strategy for treating chronic pain.

Acknowledgements

This work was supported by a grant from a Pilot Project from VCU Massey Cancer Center and National Institute on Drug Abuse (DA032246) to M.I.D. and National Institute of Health grants (GM57481) to R.L.P., (EY024717) to G.A.T. and (DA038493-01A1) to J.L.W. D.B. would like to thank The Scientific and Technical Research Council of Turkey (TUBITAK) for her postdoctoral research scholarship (2219-2013).

Author contributions

D.B. and M.I.D. designed and conducted the study, analysed the data and wrote the manuscript. D.B. and J.L.W. performed the immunohistochemistry study. S.A., W.T. and Z.G. performed part of the *in vivo* study. A.K. and G.A.T. synthesized and provided the compound. R.L.P., G.A.T. and A. H.L. elicited scientific contributions and revised the manuscript.

Conflict of interest

The authors declare no conflicts of interest.

Declaration of transparency and scientific rigour

This Declaration acknowledges that this paper adheres to the principles for transparent reporting and scientific rigour of preclinical research recommended by funding agencies, publishers and other organisations engaged with supporting research.

References

Abbott FV, Franklin KB, Westbrook RF (1995). The formalin test: scoring properties of the first and second phases of the pain response in rats. Pain 60: 91–102.

Alexander SPH, Peters JA, Kelly E, Marrion N, Benson HE, Faccenda E *et al.* (2015a). The Concise Guide to PHARMACOLOGY 2015/16: Ligand-gated ion channels. Br J Pharmacol 172: 5870–5903.

Alexander SPH, Fabbro D, Kelly E, Marrion N, Peters JA, Benson HE *et al.* (2015b). The Concise Guide to PHARMACOLOGY 2015/16: Enzymes. Br J Pharmacol 172: 6024–6109.

Bagdas D, AlSharari SD, Freitas K, Tracy M, Damaj MI (2015a). The role of alpha5 nicotinic acetylcholine receptors in mouse models of chronic inflammatory and neuropathic pain. Biochem Pharmacol 97: 590–600.

Bagdas D, Sonat FA, Hamurtekin E, Sonal S, Gurun MS (2011). The antihyperalgesic effect of cytidine-5′-diphosphate-choline in neuropathic and inflammatory pain models. Behav Pharmacol 22: 589–598.

Bagdas D, Targowska-Duda KM, López JJ, Perez EG, Arias HR, Damaj MI (2015b). The antinociceptive and antiinflammatory properties of 3-furan-2-yl-N-p-tolyl-acrylamide, a positive allosteric modulator of α7 nicotinic acetylcholine receptors in mice. Anesth Analg 121: 1369–1377.

Bernik TR, Friedman SG, Ochani M, DiRaimo R, Ulloa L, Yang H *et al.* (2002). Pharmacological stimulation of the cholinergic antiinflammatory pathway. J Exp Med 195: 781–788.

Bertrand D, Gopalakrishnan M (2007). Allosteric modulation of nicotinic acetylcholine receptors. Biochem Pharmacol 74: 1155–1163.

Booker L, Kinsey SG, Abdullah RA, Blankman JL, Long JZ, Ezzili C *et al.* (2012). The fatty acid amide hydrolase (FAAH) inhibitor PF-3845 acts in the nervous system to reverse LPS-induced tactile allodynia in mice. Br J Pharmacol 165: 2485–2496.

Chaplan SR, Bach FW, Pogrel JW, Chung JM, Yaksh TL (1994). Quantitative assessment of tactile allodynia in the rat paw. J Neurosci Methods 53: 55–63.

Curtis MJ, Bond RA, Spina D, Ahluwalia A, Alexander SP, Giembycz MA *et al.* (2015). Experimental design and analysis and their reporting: new guidance for publication in BJP. Br J Pharmacol 172: 3461–3471.

D'Amour FE, Smith DL (1941). A method for determining loss of pain sensation. J Pharmacol Exp Ther 72: 74–79.

Damaj MI, Meyer EM, Martin BR (2000). The antinociceptive effects of alpha7 nicotinic agonists in an acute pain model. Neuropharmacology 39: 2785–2791.

Davidson EM, Carlton SM (1998). Intraplantar injection of dextrorphan, ketamine or memantine attenuates formalin-induced behaviors. Brain Res 785: 136–142.

Dewey WL, Harris LS, Howes JF, Nuite JA (1970). The effect of various neurohumoral modulators on the activity of morphine and the narcotic antagonists in the tail-flick and phenylquinone tests. J Pharmacol Exp Ther 175: 435–442.

Di Cesare Mannelli L, Tenci B, Zanardelli M, Failli P, Ghelardini C (2015). α7 Nicotinic Receptor Promotes the Neuroprotective Functions of Astrocytes against Oxaliplatin Neurotoxicity. Neural Plast 2015: 396908.

Dixon WJ (1965). The up-and-down method for small samples. J Am Stat Assoc 60: 967–978.

Dziewczapolski G, Glogowski CM, Masliah E, Heinemann SF (2009). Deletion of the alpha 7 nicotinic acetylcholine receptor gene improves cognitive deficits and synaptic pathology in a mouse model of Alzheimer's disease. J Neurosci 29: 8805–8815.

Egea J, Buendia I, Parada E, Navarro E., León R, Lopez MG (2015). Anti-inflammatory role of microglial alpha7 nAChRs and its role in neuroprotection. Biochem Pharmacol 97: 463–472.

Eng LF, Ghirnikar RS, Lee YL (2000). Glial fibrillary acidic protein: GFAP-thirty-one years (1969–2000). Neurochem Res 25: 1439–1451.

Feuerbach D, Lingenhoehl K, Olpe HR, Vassout A, Gentsch C, Chaperon F *et al.* (2009). The selective nicotinic receptor α7 agonist JN403 is active in animal models of cognition, sensory gating, epilepsy and pain. Neuropharmacology 56: 254–263.

Freitas K, Carroll FI, Damaj MI (2013a). The antinociceptive effects of nicotinic receptors α7-positive allosteric modulators in murine acute and tonic pain models. J Pharmacol Exp Ther 344: 264–275.

Freitas K, Ghosh S, Ivy Carroll F, Lichtman AH, Imad Damaj M (2013b). Effects of alpha 7 positive allosteric modulators in murine inflammatory and chronic neuropathic pain models. Neuropharmacology 65: 156–164.

Freitas K, Negus S, Carroll FI, Damaj MI (2013c). In vivo pharmacological interactions between a type II positive allosteric modulator of α7 nicotinic ACh receptors and nicotinic agonists in a murine tonic pain model. Br J Pharmacol 169: 567–579.

Gao B, Hierl M, Clarkin K, Juan T, Nguyen H, Valk MV*et al.* (2010). Pharmacological effects of nonselective and subtype-selective nicotinic acetylcholine receptor agonists in animal models of persistent pain. Pain 149: 33–49.

Gao YJ, Ji RR (2010). Targeting astrocyte signaling for chronic pain. Neurotherapeutics 7: 482–493.

Gill J, Dhankher P, Sheppard T, Sher E, Millar N (2012). A series of α7 nicotinic acetylcholine receptor allosteric modulators with close chemical similarity but diverse pharmacological properties. Mol Pharmacol 81: 710–718.

Gill JK, Savolainen M, Young GT, Zwart R, Sher E, Millar NS (2011). Agonist activation of alpha7 nicotinic acetylcholine receptors via an allosteric transmembrane site. Proc Natl Acad Sci U S A 108: 5867–5872.

Girod R, Crabtree G, Ernstrom G, Ramirez-Latorre J, McGehee D, Turner J *et al.* (1999). Heteromeric complexes of α5 and/or α7 subunits. Effects of calcium and potential role in nicotine-induced presynaptic facilitation. Ann N Y Acad Sci 868: 578–590.

Hamurtekin E, Gurun MS (2006). The antinociceptive effects of centrally administered CDP-choline on acute pain models in rats: the involvement of cholinergic system. Brain Res 1117: 92–100.

Horenstein NA, Papke RL, Kulkarni AR, Chaturbhuj GU, Stokes C, Manther K *et al.* (2016). Critical molecular determinants of α7 nicotinic acetylcholine receptor allosteric activation: separation of direct allosteric activation and positive allosteric modulation. J Biol Chem. doi:10.1074/jbc.M115.692392.

Hurst RS, Hajós M, Raggenbass M, Wall TM, Higdon NR, Lawson JA *et al.* (2005). A novel positive allosteric modulator of the alpha7 neuronal nicotinic acetylcholine receptor: in vitro and in vivo characterization. J Neurosci 25: 4396–4405.

Hylden JL, Wilcox GL (1980). Intrathecal morphine in mice: a new technique. Eur J Pharmacol 67: 313–316.

Ji RR, Gereau RW IV, Malcangio M, Strichartz GR (2009). MAP kinase and pain. Brain Res Rev 60: 135–148.

Ji R-R, Suter MR (2007). p38 MAPK, microglial signaling, and neuropathic pain. Mol Pain 3: 33.

Kilkenny C, Browne W, Cuthill IC, Emerson M, Altman DG (2010). Animal research: reporting in vivo experiments: the ARRIVE guidelines. Br J Pharmacol 160: 1577–1579.

Kim DS, Figueroa KW, Li KW, Boroujerdi A, Yolo T, David Luo Z (2009). Profiling of dynamically changed gene expression in dorsal root ganglia post peripheral nerve injury and a critical role of injury-induced glial fibrillary acetic protein in maintenance of pain behaviors. Pain 143: 114–122.

Kulkarni AR, Thakur GA (2013). Microwave-assisted expeditious and efficient synthesis of cyclopentene ring-fused tetrahydroquinoline derivatives using three-component povarov reaction. Tetrahedron Lett 54. doi:10.1016/j.tetlet.2013.09.107.

Liu Y, Hu J, Wu J, Zhu C, Hui Y, Han Y*et al.* (2012). α7 nicotinic acetylcholine receptor-mediated neuroprotection against dopaminergic neuron loss in an MPTP mouse model via inhibition of astrocyte activation. J Neuroinflammation 9: 98.

McGrath JC, Lilley E (2015). Implementing guidelines on reporting research using animals (ARRIVE etc.): new requirements for publication in BJP. Br J Pharmacol 172: 3189–3193.

Moon JY, Roh DH, Yoon SY, Choi SR, Kwon SG, Choi HS *et al.* (2014). σ1 receptors activate astrocytes via p38 MAPK phosphorylation leading to the development of mechanical allodynia in a mouse model of neuropathic pain. Br J Pharmacol 171: 5881–5897.

Munro G, Hansen RR, Erichsen HK, Timmermann DB, Christensen JK, Hansen HH (2012). The α7 nicotinic ACh receptor agonist compound B and positive allosteric modulator PNU-120596 both alleviate inflammatory hyperalgesia and cytokine release in the rat. Br J Pharmacol 167: 421–435.

Niranjan R, Nath C, Shukla R (2012). Melatonin attenuated mediators of neuroinflammation and alpha-7 nicotinic acetylcholine receptor mRNA expression in lipopolysaccharide (LPS) stimulated rat astrocytoma cells, C6. Free Radic Res 46: 1167–1177.

Nizri E, Irony-Tur-Sinai M, Lory O, Orr-Urtreger A, Lavi E, Brenner T (2009). Activation of the cholinergic anti-inflammatory system by nicotine attenuates neuroinflammation via suppression of Th1 and Th17 responses. J Immunol 183: 6681–6688.

Papke RL, Bagdas D, Kulkarni AR, Gould T, AlSharari SD, Thakur GA *et al.* (2015). The analgesic-like properties of the alpha7 nAChR silent agonist NS6740 is associated with non-conducting conformations of the receptor. Neuropharmacology 91: 34–42.

Papke RL, Chojnacka K, Horenstein NA (2014a). The minimal pharmacophore for silent agonism of alpha7 nAChR. J Pharmacol Exp Ther 350: 665–680.

Papke RL, Horenstein NA, Kulkarni AR, Stokes C, Corrie LW, Maeng CY*et al.* (2014b). The activity of GAT107, an allosteric activator and positive modulator of α7 nicotinic acetylcholine receptors (nAChR), is regulated by aromatic amino acids that span the subunit interface. J Biol Chem 289: 4515–4531.

Parada E, Egea J, Buendia I, Negredo P, Cunha AC, Cardoso S *et al.* (2013). The microglial α7-acetylcholine nicotinic receptor is a key element in promoting neuroprotection by inducing heme oxygenase-1 via nuclear factor erythroid-2-related factor 2. Antioxid Redox Signal 19: 1135–1148.

Paulo JA, Brucker WJ, Hawrot E (2009). Proteomic analysis of an alpha7 nicotinic acetylcholine receptor interactome. J Proteome Res 8: 1849–1858.

Schreiber KL, Beitz AJ, Wilcox GL (2008). Activation of spinal microglia in a murine model of peripheral inflammation-induced, long-lasting contralateral allodynia. Neurosci Lett 440: 63–67.

Shen JX, Yakel JL (2012). Functional alpha7 nicotinic ACh receptors on astrocytes in rat hippocampal CA1 slices. J Mol Neurosci 48: 14–21.

Shytle RD, Mori T, Townsend K, Vendrame M, Sun N, Zeng J *et al.* (2004). Cholinergic modulation of microglial activation by α7 nicotinic receptors. J Neurochem 89: 337–343.

de Simone R, Ajmone-Cat MA, Carnevale D, Minghetti L (2005). Activation of α7 nicotinic acetylcholine receptor by nicotine selectively up-regulates cyclooxygenase-2 and prostaglandin E2 in rat microglial cultures. J Neuroinflammation 2: 4.

Southan C, Sharman JL, Benson HE, Faccenda E, Pawson AJ, Alexander SP *et al.* (2016). The IUPHAR/BPS Guide to PHARMACOLOGY in 2016: towards curated quantitative interactions between 1300 protein targets and 6000 ligands. Nucl. Acids Res. 44: D1054–D1068.

Stokes C, Treinin M, Papke RL (2015). Looking below the surface of nicotinic acetylcholine receptors. Trends Pharmacol Sci 36: 514–523.

Su X, Jae WL, Matthay ZA, Mednick G, Uchida T, Fang X *et al.* (2007). Activation of the α7 nAChR reduces acid-induced acute lung injury in mice and rats. Am J Respir Cell Mol Biol 37: 186–192.

Takeda D, Nakatsuka T, Gu JG, Yoshida M (2007). The activation of nicotinic acetylcholine receptors enhances the inhibitory synaptic transmission in the deep dorsal horn neurons of the adult rat spinal cord. Mol Pain 3: 26.

Thakur GA, Kulkarni AR, Deschamps JR, Papke RL (2013). Expeditious synthesis, enantiomeric resolution, and enantiomer functional characterization of (4-(4-bromophenyl)-3a,4,5,9b-tetrahydro-3H-cyclopenta[c]quinoline-8-sulfonamide (4BP-TQS): an allosteric agonist-positive allosteric modulator of α7 nicotinic ac. J Med Chem 56: 8943–8947.

Thomsen MS, Hansen HH, Timmerman DB, Mikkelsen JD (2010). Cognitive improvement by activation of alpha7 nicotinic acetylcholine receptors: from animal models to human pathophysiology. Curr Pharm Des 16: 323–343.

Timmermann DB, Grønlien JH, Kohlhaas KL, Nielsen EØ, Dam E, Jørgensen TD *et al.* (2007). An allosteric modulator of the α7 nicotinic acetylcholine receptor possessing cognition-enhancing properties in vivo. J Pharmacol Exp Ther 323: 294–307.

Umana IC, Daniele CA, McGehee DS (2013). Neuronal nicotinic receptors as analgesic targets: it's a winding road. Biochem Pharmacol 86: 1208–1214.

Wang Y, Su DM, Wang RH, Liu Y, Wang H (2005). Antinociceptive effects of choline against acute and inflammatory pain. Neuroscience 132: 49–56.

Wilkerson JL, Gentry KR, Dengler EC, Wallace JA, Kerwin AA, Armijo LM *et al.* (2012a). Intrathecal cannabilactone CB 2R agonist, AM1710, controls pathological pain and restores basal cytokine levels. Pain 153: 1091–1106.

Wilkerson JL, Gentry KR, Dengler EC, Wallace JA, Kerwin AA, Kuhn MN *et al.* (2012b). Immunofluorescent spectral analysis reveals the intrathecal cannabinoid agonist, AM1241, produces spinal anti-inflammatory cytokine responses in neuropathic rats exhibiting relief from allodynia. Brain Behav 2: 155–177.

Williams DK, Wang J, Papke RL (2011). Positive allosteric modulators as an approach to nicotinic acetylcholine receptor-targeted therapeutics: advantages and limitations. Biochem Pharmacol 82: 915–930.

Yang Y-H, Li D-L, Bi X-Y, Sun L, Yu X-J, Fang H-L *et al.* (2015). Acetylcholine inhibits LPS-induced MMP-9 production and cell migration via the a7 nAChR-JAK2/STAT3 pathway in RAW264.7 cells. Cell Physiol Biochem 36: 2025–2038.

Supporting Information

Additional Supporting Information may be found in the online version of this article at the publisher's web-site:

http://dx.doi.org/10.1111/bph.13528

Figure S1 Low power staining in spinal cord. (A) Image taken at 5× magnification of GFAP fluorescent staining in mouse lumbar spinal cord treated with CFA–vehicle. (B) Image taken at 5× magnification of p-p38MAPK fluorescent staining in mouse lumbar spinal cord treated with CFA–-vehicle. Scale bar is equal to 200 μm.